

Quantum accelerator modes: A tool for atom optics

R. M. Godun, M. B. d'Arcy, M. K. Oberthaler* G. S. Summy, and K. Burnett

Clarendon Laboratory, Department of Physics, University of Oxford, Parks Road, Oxford, OX1 3PU, United Kingdom

(Received 21 December 1999; published 14 June 2000)

We describe an atom-optical technique for producing large changes in the momentum of cold atoms using a pulsed standing wave of off-resonant light. Experimental results are presented showing how the efficiency and the amount of momentum transfer depend on the parameters of the light field. We also present a theoretical analysis and derive a closed formula which is in excellent agreement with the experimental data.

PACS number(s): 42.50.Vk, 03.75.-b

I. INTRODUCTION

Controlling the momentum and position of ultracold atoms has received wide interest throughout the world in the last two decades. The name ‘‘atom optics’’ was coined for this field because it involves the coherent manipulation of atomic de Broglie waves [1,2]. The ability to perform atom optics is crucial to the development of devices and processes that use atomic de Broglie waves. Lithography [3], atom interferometry [4], and the atom laser [5] all require one to have precise control over the external motion of atoms.

There have been a number of methods that have demonstrated this control. These can essentially be divided into three groups: those using nanofabricated matter gratings [6], those using static magnetic fields [7], and those using light. In general the last category has proved to be the most widely used because of the relative ease with which the necessary optical potentials can be realized to achieve coherent momentum transfer. For example, methods using Raman pulses [8], adiabatic transfer [9,10], evanescent waves [11], and diffraction from an off-resonant standing light wave [12] have all been demonstrated as methods for imparting photon momenta to atoms. It has proved difficult to scale these processes (by applying more pulses, for example) either because of their efficiency [13] or for technical reasons.

What is needed is a technique that uses light to create with high efficiency an almost arbitrarily large change in the momentum of an atom. The quantum accelerator mode [14] that we have recently demonstrated can fulfill this requirement.

The principle of an accelerator mode is that by exposing particles to a pulsed sinusoidal potential they gain momentum. Particles with a certain initial velocity are given an identical ‘‘kick’’ by the potential every time it is pulsed on. In our experimental arrangement, atoms that are dropped from a magneto-optic trap (MOT) experience a pulsed sinusoidal potential, generated by a standing wave of off-resonant light. Some of these atoms have initial velocities that allow them to enter an accelerator mode. Typical experimental data showing the atomic momentum distributions after different numbers of pulses of the potential are shown in Fig. 1. It can clearly be seen that a class of atoms accelerates

out from the main distribution, gaining momentum with every pulse. These atoms are in an accelerator mode, which is analogous to a child being pushed on a swing. Repeated pushes at the correct interval allow the child to gain more and more momentum and thus accelerate. If the pushes are mistimed, the child’s momentum can be increased or decreased so that, although in general the child may accelerate for a few pushes, the net result is very little acceleration. In our experiment, we are dealing with cold atoms and not classical particles so we expect some modification to this simple picture.

In this paper, we derive the theoretical condition for a classical accelerator mode and build on this to obtain the condition in the quantum case. After a discussion of our experimental setup, we go on to show in detail how the accelerator mode can be controlled by the precise nature of the standing light wave that creates it. Finally we look at evidence for the coherence of these accelerator modes and discuss their potential as an atom-optical beam splitter.

II. THEORY

A. The classical accelerator mode

To gain an understanding of the accelerator mode, we look first at the classical dynamics depicted in Fig. 2. We consider a particle moving in a vertical sinusoidal potential which is periodically switched on and off. In addition to the force of gravity, the particle will experience a force from the potential and a consequent momentum change if it is located in a region where the gradient of the potential is nonzero. We assume that the particle is initially placed at a position where it can experience a momentum change. We also assume that the particle does not move a significant distance within the potential during the time of a pulse. If the potential is given by $U = (U_{\max}/2)[1 + \cos(Gx)]$, where $2\pi/G$ is the spatial period λ_G of the potential, the momentum change in a pulse is $\Delta p = -\nabla U \Delta t$, where Δt is the length of the pulse. The velocity imparted by each pulse will then be

$$v_R = \frac{U_{\max}}{2m} \sin(Gx) G \Delta t. \quad (1)$$

Only if the particle receives the same kick from every pulse will its momentum increase linearly with pulse number and the particle remain in an accelerator mode. To find such a classical accelerator mode, we need to determine if there is

*Present address: Universität Konstanz, Fachbereich Physik, Universitätsstrasse 10, D-78457 Konstanz, Germany.

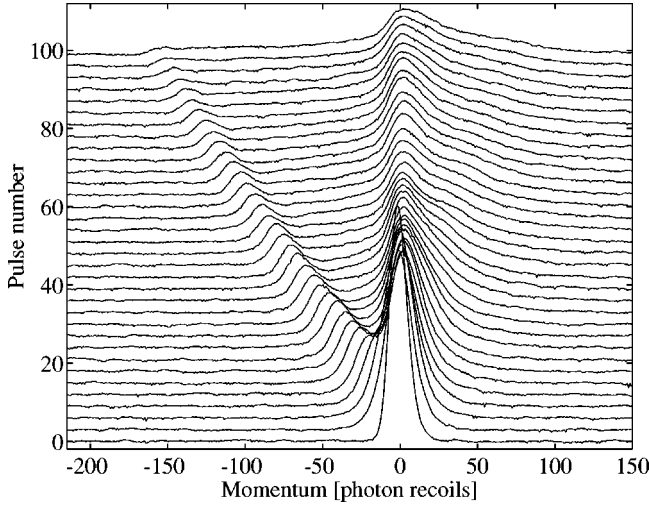


FIG. 1. Experimental atomic momentum distributions for different numbers of standing light wave pulses. The peak that is accelerating away from the central distribution corresponds to atoms in an accelerator mode. The data have been averaged over 10 shots.

a particular value of the time between pulses, T , where the particle always returns to the same position within a period of the potential. In other words we need to find a value of T for which the distance the particle moves between successive pulses, s , is an integer number of spatial periods of the sinusoidal potential. This is equivalent to the condition

$$s = (N_p l' + l) \lambda_G, \quad (2)$$

where l and l' are integers and N_p is the number of the pulse. Note that the integer multiple has been split into a factor dependent on pulse number and a separate factor, independent of pulse number. This distance can be calculated from classical mechanics. At the time of the N_p th pulse $t = (N_p - 1)T$, so that the velocity gained due to the gravitational acceleration is $v_g = v_i + g(N_p - 1)T$. The velocity gained from the kicks of the potential is $v_k = N_p v_R$. Thus between the N_p th and $(N_p + 1)$ th pulse the particle moves a distance

$$s = (gT^2 + v_R T) N_p + (v_i T - \frac{1}{2} g T^2). \quad (3)$$

Equating this to Eq. (2), we find that for an accelerator mode,

$$gT^2 + v_R T = l' \lambda_G \quad (4)$$

and

$$v_i T - \frac{1}{2} g T^2 = l \lambda_G. \quad (5)$$

Hence we can find the pulse separation times T for which a certain initial velocity class v_i is continually kicked onto the same gradient of the potential. These particles will gain momentum linearly with pulse number and are in a long-lived accelerator mode.

B. The quantum accelerator mode

The quantum accelerator mode is the quantum mechanical analog of the above idea. Cold atoms are used instead of the

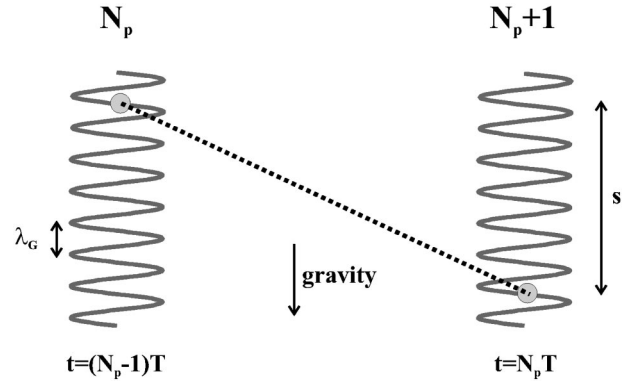


FIG. 2. A schematic of the classical situation, with time increasing to the right. The distance s through which the particle moves between pulses must be a whole multiple of the spatial period of the potential for the particle to remain in an accelerator mode.

classical particles and the sinusoidal potential can be created with a standing wave of off-resonant light. The laser-cooled atoms that participate in the accelerator mode cannot be treated classically but can be thought of as de Broglie wave packets spread out over many periods of the potential. Thus we consider each pulse of the standing light wave as a phase grating which diffracts the atomic de Broglie waves into a series of diffraction orders, as shown in Fig. 3.

Through the light shift, the standing wave creates a potential of the form

$$U(x, t) = \frac{U_{\max}}{2} [1 + \cos(Gx)] \sum_{N_p} \delta(t - N_p T) \quad (6)$$

with the grating vector $G = 2k$ where k is the light wave vector, T is the time between the pulses, and N_p is the pulse number. The δ function expresses the fact that the time for which a pulse is applied is much shorter than the time between the pulses. This potential changes the spatial phase of an atomic wave incident on it by $\phi(x) = -U(x)\Delta t/\hbar$ where Δt is the interaction time. Since the pulse length is assumed to be very short the movement of the atom during the interaction is negligible. The atom is thus in the Raman-Nath regime and the standing light wave acts as a thin phase diffraction grating.

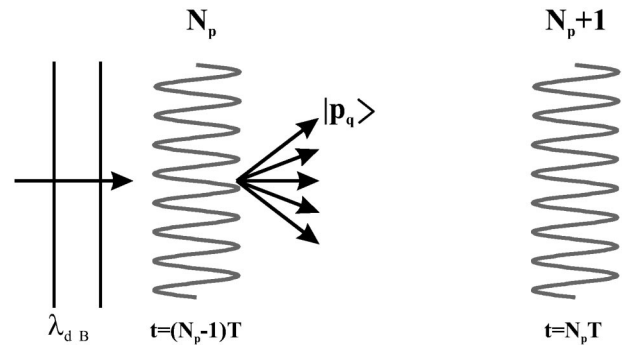


FIG. 3. A schematic of the quantum situation, with time increasing to the right. The potential behaves as a thin phase grating and diffracts the incident de Broglie wave. Several adjacent momentum states must rephase for an accelerator mode to exist.

If one imagines a plane atomic wave incident upon such a potential, the resulting output will be composed of an array of different diffraction orders. That is,

$$|\psi\rangle = \sum_{n=-\infty}^{\infty} i^n J_n(\phi_d) |p_n\rangle, \quad (7)$$

where J_n is the n th order Bessel function of the first kind, $\phi_d = U_{\max} \Delta t / (2\hbar)$ is the phase modulation depth of the grating, and $|p_n\rangle$ represents a momentum state after one grating with momentum in the grating direction of $p = n\hbar G$. The Bessel function $J_n(\phi_d)$ has its maximum when $\phi_d \sim n + 1$; thus the order diffracted with the highest probability is given roughly by $n_{\max} \approx (\phi_d - 1)$. This corresponds to a most likely momentum after one grating of $n_{\max} \hbar G$.

To find an accelerator mode in the quantum case, we are looking for a condition on the pulse separation T and the initial velocity v_i that will cause part of the atomic wave field to replicate itself from grating to grating. Such a mode, with the same form at every pulse, should have a fixed phase relationship between its constituent components at the time of each pulse. To avoid ambiguity between the labeling of diffraction orders after a particular pulse and the total momentum accumulated after several pulses, we introduce a new parameter q . This represents the total number of grating recoils, $\hbar G$, that the accelerator mode has gained up to and including the N_p th pulse. The phase accumulated in the momentum state $|p_q\rangle$, relative to that accumulated in the state $|p_{q=0}\rangle$, during the free evolution between the N_p th and $(N_p + 1)$ th pulse is

$$\phi_q = \frac{\hbar G^2}{2m} T q^2 + v_i G T q + g G T^2 N_p q, \quad (8)$$

where m is the atomic mass. The atoms also accumulate an interaction phase at the grating, as shown by the factor i^n in Eq. (7). The state $|p_q\rangle$ has a total interaction phase i^q , which depends only on the value of q and not on how $|p_q\rangle$ was reached through the diffraction orders at previous pulses.

From one pulse to the next, the accumulated phase difference between two adjacent momentum states is thus found to be

$$\phi_q - \phi_{q-1} = \frac{\hbar G^2}{2m} T(2q-1) + v_i G T + g G T^2 N_p. \quad (9)$$

We see from this expression that the presence of gravity prohibits the simultaneous rephasing of *all* the momentum orders at any time after a pulse. The accelerator mode itself consists of only a few momentum states and it is sufficient in our analysis to follow the behavior of only these states. For the accelerator mode to replicate itself at every pulse the free evolution phases of these states must rephase in the interval between every pulse. This requires the phase differences $\phi_q - \phi_{q-1}$ to be as close as possible to whole multiples of 2π . Just as in the classical case, Eq. (9) now gives a rephasing condition, which can be separated into Eq. (10), contain-

ing q and N_p which increase linearly with pulse number, and Eq. (11), containing terms that have no pulse number dependence:

$$\frac{\hbar G^2}{2m} T 2q + g G T^2 N_p = 2\pi q l' \quad (10)$$

and

$$v_i G T - \frac{\hbar G^2}{2m} T = 2\pi l, \quad (11)$$

where l and l' are integers. The first of these allows a calculation of the time interval between the pulses and with the second the initial velocity can be found.

To express these solutions more concisely, we introduce a scaled time

$$T = \alpha T_{1/2} \quad \text{with} \quad T_{1/2} = \frac{2\pi m}{\hbar G^2}, \quad (12)$$

where $T_{1/2}$ is $66.5 \mu\text{s}$ for cesium in light of 895 nm . Equations (10) and (11) now become

$$\alpha^2 + \frac{q}{N_p} \gamma \alpha - \frac{q l'}{N_p} \gamma = 0 \quad (13)$$

and

$$v_i = \left(\frac{l}{\alpha} + \frac{1}{2} \right) \frac{\hbar G}{m} \quad (14)$$

with $\gamma = \hbar^2 G^3 / 2\pi m^2 g$, which is approximately 10 for cesium with 895 nm light.

Solving Eq. (13) gives

$$q = \frac{N_p}{\gamma} \frac{\alpha^2}{l' - \alpha}. \quad (15)$$

Thus the momentum of the accelerator mode after N_p pulses separated by $\alpha T_{1/2}$ is $q \hbar G$. Note that without gravity, $1/\gamma = 0$ and the accelerator mode ceases to exist.

We can also see that

$$\phi_{q+1} - \phi_q = \phi_q - \phi_{q-1} + 2\pi \alpha. \quad (16)$$

This implies that if α is set to a near-integer value, where $|p_q\rangle$ and its neighbor $|p_{q-1}\rangle$ are in phase, then $|p_q\rangle$ and its other neighbor $|p_{q+1}\rangle$ are not perfectly in phase. As α takes values further from an integer, $|p_q\rangle$ and $|p_{q+1}\rangle$ become increasingly out of phase, eventually destroying the possibility of an accelerator mode. This restriction on α means that accelerator modes can be formed only when the pulse separation time T is close to integer values of $T_{1/2}$.

Figure 4 shows the remarkable accuracy of this simple analysis. The dashed curve is Eq. (15) for $l' = 1$ with no fit parameters. The underlying experimental data show the measured momentum distributions with a pulse length of $0.5 \mu\text{s}$.

Note that q can take only integer values so the momentum transferred is quantized. This is not observed in the results

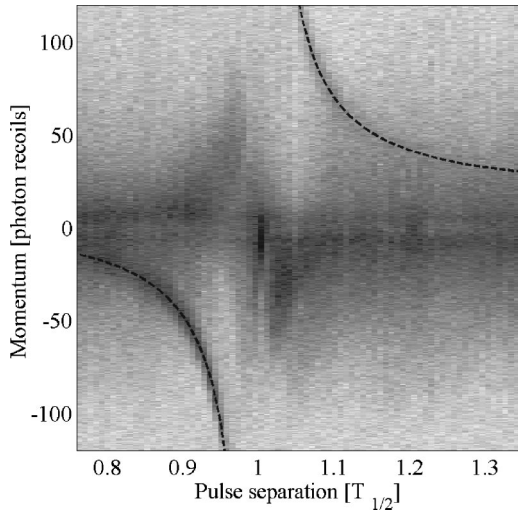


FIG. 4. The experimental data, averaged over 10 shots, show momentum distributions obtained after 30 pulses with different pulse separations close to $T_{1/2}$, where our experimental parameters set $T_{1/2}$ equal to $66.5 \mu\text{s}$. Each pulse of the standing light wave was on for $0.5 \mu\text{s}$. The dashed curve is Eq. (15) for $l'=1$ with no fit parameters, i.e., $2q=2 \times 30\alpha^2/\gamma(1-\alpha)$, where the factor of 2 arises from plotting in units of $\hbar k$ instead of $\hbar G$.

because the final momentum is measured over an ensemble of atoms with a range of initial velocities. In contrast, the momentum transfer in the classical case is not quantized and can be tuned continuously. Note also that, in the quantum case, the modulation depth of the potential, ϕ_d , does not determine the final momentum gained; this is fixed by α , the scaled time. The role of ϕ_d is only to determine the relative populations in the diffraction orders produced at each grating. For a particular α only certain diffraction orders take part in the formation of an accelerator mode and ϕ_d affects only the efficiency with which these orders are populated. This is different from the classical case where Eq. (4) shows that the pulse separation depends on the recoil velocity, which changes with the modulation depth of the potential.

Equation (14) tells us that accelerator modes, which occur for values of α close to 1, select atoms in an initial velocity class close to half-integer values of the grating recoil velocity $\hbar G/m$.

III. EXPERIMENTAL SETUP

The quantum accelerator modes described above were observed with laser-cooled cesium atoms in a standing light wave. As shown in Fig. 5, the standing light wave was formed from a vertically propagating Ti:sapphire laser beam. The light was typically detuned 6 GHz below the $D1(6^2S_{1/2} \rightarrow 6^2P_{1/2})F=4 \rightarrow F'=3$ transition in cesium, as shown in Fig. 6. The beam itself had a full width half maximum diameter of $\sim 1.5 \text{ mm}$ and the power was approximately 250 mW. The pulses were switched on and off with an acousto-optic modulator driven by a fast rf amplitude modulator. A phase shifter was also situated in the light beam to allow the standing wave to have different phases. This was used to enhance or even cancel the effect of grav-

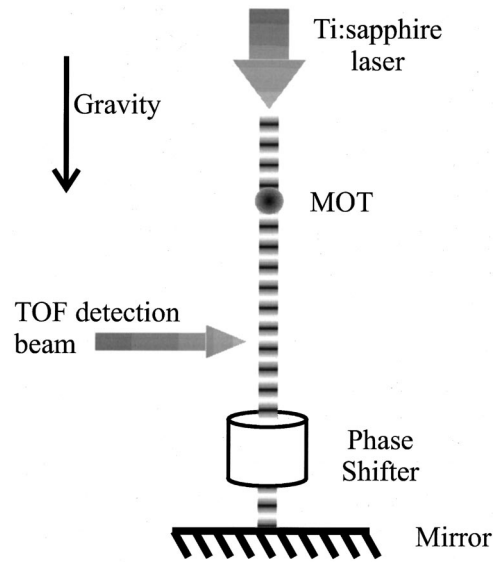


FIG. 5. The experimental setup with a pulsed, vertical standing light wave formed from the retroreflection of a Ti:sapphire laser beam. The atomic source was a MOT and the atomic momentum distribution was measured 50 cm below the trap position with a time of flight (TOF) technique. The phase shifter allowed the realization of different accelerations of the atoms relative to the standing wave.

ity, as described in the next section.

The atomic source was a MOT of typically 10^7 cesium atoms at a temperature of about $5 \mu\text{K}$ after molasses cooling. The atoms were released from the trap and after 5 ms the standing light wave pulses were applied. The atoms were detected 50 cm below, as they fell through a $50 \mu\text{W}$ probe beam, 15 mm wide and 2 mm thick. This probe beam was on resonance at the $D2(6^2S_{1/2} \rightarrow 6^2P_{3/2})F=4 \rightarrow F''=5$ transition so that the amount of absorption was proportional to the number of atoms in the $F=4$ state. By measuring the time of

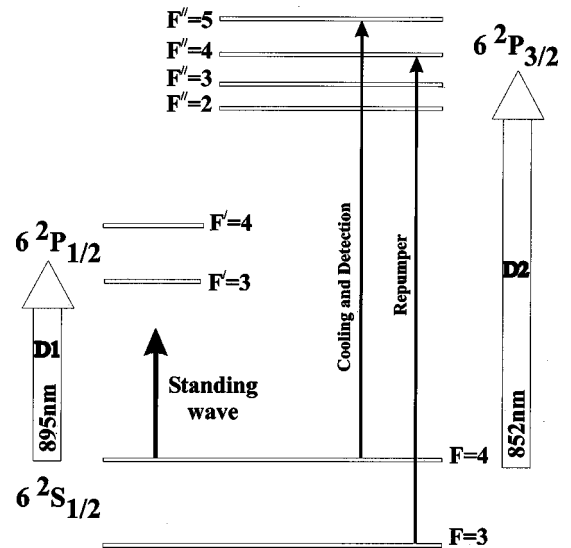


FIG. 6. The cesium atomic levels used in the experiment, with the relevant transitions marked.

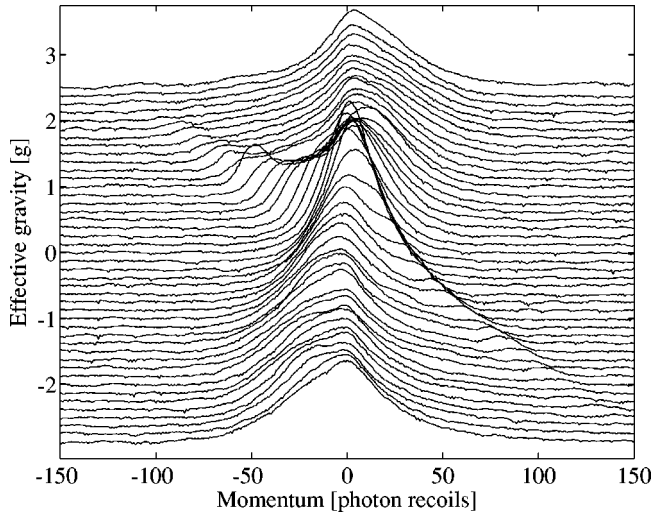


FIG. 7. The momentum distributions after 30 pulses separated by a time of $T=60 \mu\text{s}$, where the phase shifter was used to simulate effective gravitational accelerations between $\pm 2.5g$. The phase shifter allowed both positive and negative momentum kicks to be realized, thus giving full control over the final momentum distribution. The laser light was 6 GHz red detuned and the pulses, of length $0.5 \mu\text{s}$, had an intensity in the standing wave of 28 W/cm^2 . The data have been averaged over 10 shots.

flight, the momentum distribution of the atoms could be determined.

IV. THE ROLE OF GRAVITY

It can be seen from Eq. (10) that changing N_p will affect the rephasing of adjacent momentum states $|p_q\rangle$ and $|p_{q-1}\rangle$. If N_p is increased, the rephasing of momentum states with higher q will be favored. This is as expected since increasing the pulse number increases the momentum of the accelerator mode, as seen in Fig. 1. Since g and N_p occur as a product in one of the terms of Eq. (10), it should be expected that increasing gravity instead of N_p would also change the momentum of the accelerator mode linearly. Obviously gravity cannot be changed directly, but it is possible to change the acceleration of the atoms relative to the standing wave. This is achieved by using the phase shifter to adjust the phase of the standing wave quadratically with pulse number. An adjustment in phase is equivalent to translating the whole standing wave along its length. In this way, the gravitational acceleration could be canceled, for example, by shifting the standing wave such that at each pulse the atoms found themselves at the position on the standing wave where they would have been in the absence of falling. By controlling the amount by which the standing light wave is shifted, a wide range of effective gravitational accelerations can be realized.

The results of such experiments, where the effective gravitational acceleration was varied between $\pm 2.5g$ for 30 pulses separated by $T=60 \mu\text{s}$, are shown in Fig. 7. It can be clearly seen that the momentum change is linear with effective acceleration, just as it is with pulse number. This plot shows the control that can be exercised over the momentum distribution and how the atoms can be made to both accel-

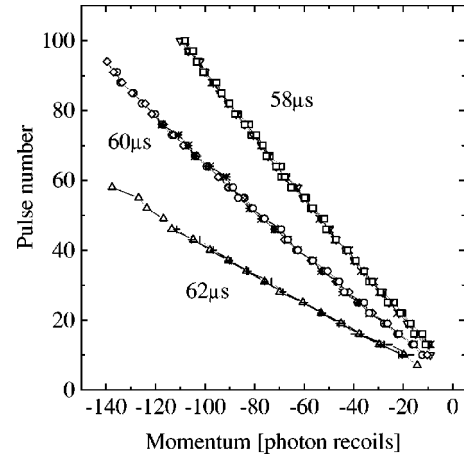


FIG. 8. The graph shows the linear momentum change of the accelerator mode with pulse number for three different pulse separations and at four different intensities: 25.4 , 23.8 , 21.6 , and 16.4 W/cm^2 . Note how for each pulse separation time the accelerator mode's momentum is the same for all intensities. The standing light wave was 6 GHz red detuned.

erate and decelerate. This is an important property in attempting to implement the accelerator mode as, for example, part of an interferometer. Looking carefully at the data, it can be seen that, when the effective gravitational acceleration was equal to g , the number of atoms in the accelerator mode was slightly larger. This is because the phase shifter was not used for this trace so there was less disturbance to the standing wave and the efficiency of the accelerator mode was improved. It is noteworthy that, since the phase shifter can simulate the effect of an external acceleration of the atoms relative to the standing light wave, all of the experiments described here could also be performed with a horizontal standing light wave.

V. THE DEPENDENCE OF THE ACCELERATOR MODE ON THE LIGHT FIELD

Having seen that the accelerator mode has the potential to be a very useful tool in atom optics, it is important to characterize its behavior. We now consider the effects of the intensity, detuning, and polarization of the light field on the accelerator mode.

A. Intensity

From the discussion in Sec. II B, it is seen that the accelerator mode arises from diffraction into orders which are specified by the rephasing condition for a given pulse separation time. We expect that for a particular pulse separation, the quantum accelerator mode acquires a momentum that is independent of the intensity of the light field. This behavior is seen very clearly in Fig. 8. This shows the momentum change of the accelerator mode, just as in Fig. 1, for increasing pulse number with four different intensities at each of three pulse separation times. As predicted, the momentum changes for a given pulse separation time are independent of the intensity. The effect of the intensity is to alter the effi-

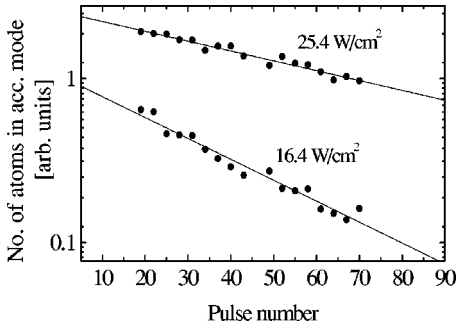


FIG. 9. The number of atoms in the accelerator mode with increasing pulse number for two different intensities of the standing light wave. The pulses were separated by $60 \mu\text{s}$ and the light was 6 GHz red detuned. The vertical axis is plotted logarithmically so the linear change with pulse number represents an exponential decay in efficiency. This demonstrates a fixed probability per pulse of remaining in the accelerator mode of 99.1% and 96.8% for the higher and lower intensity data, respectively.

ciency with which the atoms are diffracted into orders that rephase and form the accelerator mode. This relates to the discussion of the relative amplitudes in each diffraction order after a grating. To populate most efficiently the orders that will create the accelerator modes, $n \sim q/N_p$, it is necessary to choose an intensity where $\phi_d \sim n + 1$. The effect of two different intensities on the number of atoms in an accelerator mode is plotted in Fig. 9 for increasing numbers of pulses. Note that the vertical scale is logarithmic, so the straight line fits show that the efficiency decreases exponentially with pulse number. This is consistent with a fixed probability per pulse of diffracting into the desired orders.

B. Detuning

The detuning of the light field can also be adjusted. For detunings of ~ 6 GHz, the effect of increasing the detuning further is to reduce the modulation depth ϕ_d of the standing wave and, as with intensity, affect the number of atoms in the accelerator mode without changing the momentum of the accelerator mode. Decreasing the detunings and bringing the light closer to resonance, however, will increase another effect: spontaneous emission. This causes atoms to be lost from the system, thus reducing the overall signal size. These features can be seen in Fig. 10 which shows the experimental results for the momentum distributions after 30 pulses of standing light waves with different detunings.

Note that positive and negative detunings have the same effect and in each case the accelerator mode's momentum has the same sign and magnitude. This is because the kick direction arises from the particular diffraction orders that rephase and these have no dependence on the sign of the detuning.

It can be seen in Fig. 10 that the accelerator mode is suppressed more for small positive detunings than for small negative detunings. This feature is simply due to the existence of another hyperfine level, $F' = 4$, at +1 GHz from the upper level in the reference transition as seen in Fig. 6. It is for this reason that we choose to red detune the standing light wave to create accelerator modes.

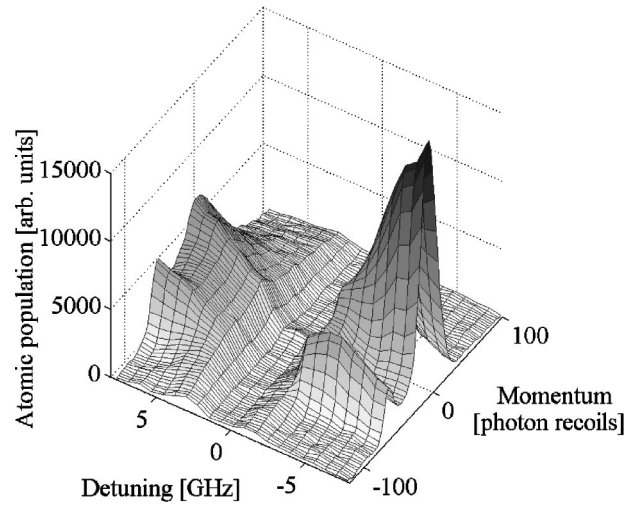


FIG. 10. The momentum distributions after 30 pulses, separated by $60 \mu\text{s}$, are shown for different detunings of the standing light wave. The momentum of the accelerator mode is independent of the detuning, and even the sign of the detuning does not affect the imparted momentum. The disappearance of the atoms close to resonance is due to the effect of spontaneous emission which reduces the number of atoms in the detected state. The data have been averaged over 10 shots.

C. Polarization

Another parameter of the light field that can easily be adjusted is its polarization. Figure 11 shows the experimental results of the accelerator mode for linear, elliptical, and circular polarizations.

We see that the accelerator mode favors linear polarizations. An explanation for this comes from the fact that the atoms which undergo acceleration are in many magnetic sub-levels of the ground level $F = 4$. In the $D1$ transition in cesium, there are two upper levels, $F' = 3$ and $F' = 4$, sepa-

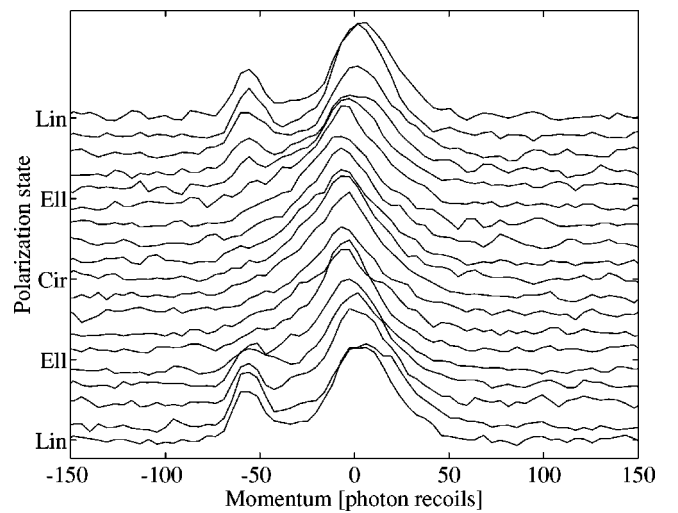


FIG. 11. Momentum distributions after 30 pulses separated by $60 \mu\text{s}$, as the polarization of the standing wave is changed from linear to circular and back to linear. Single-shot data were recorded and then smoothed by averaging over three adjacent momentum points throughout the distributions.

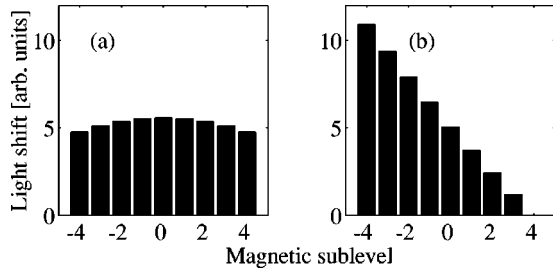


FIG. 12. The relative light shifts of the magnetic sublevels that participate in the accelerator mode are shown for (a) linearly polarized light and (b) circularly polarized light. The constancy of the light shift across the levels in case (a) allows the accelerator mode to exist. In case (b), the light shifts vary so much that different magnetic sublevels experience different modulation depths of the standing wave. This results in a whole range of diffraction orders becoming populated after each grating and so no clear accelerator mode is seen.

rated by 1 GHz. The periodic kicking potential comes from the sum of the light shifts of each of these two levels. It so happens that in cesium the total light shift is almost constant across the ground magnetic sublevels for linearly polarized light. For circularly polarized light, however, the magnetic sublevels receive shifts differing by up to a factor of 3. These shifts are shown in Fig. 12. Thus in circularly polarized light atoms in different magnetic sublevels will experience periodic potentials with a wide range of modulation depths ϕ_d . This can lead to a reduction of population in the orders that are able to satisfy the conditions for an accelerator mode.

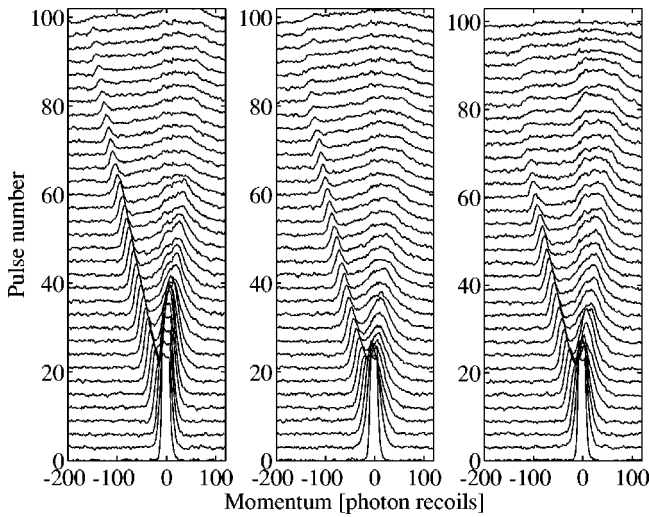


FIG. 13. The momentum distributions with increasing pulse number are plotted for differing pulse lengths of 0.5, 0.6, and 0.7 μs from left to right. The necessity of being in the Raman-Nath regime is demonstrated by the fact that the accelerator mode dies away at lower momenta for longer pulse lengths. These results are all for a standing wave of light with intensity 25.4 W/cm^2 , 6 GHz red detuned, and with pulses separated by 60 μs . The data were averaged over 5 shots.

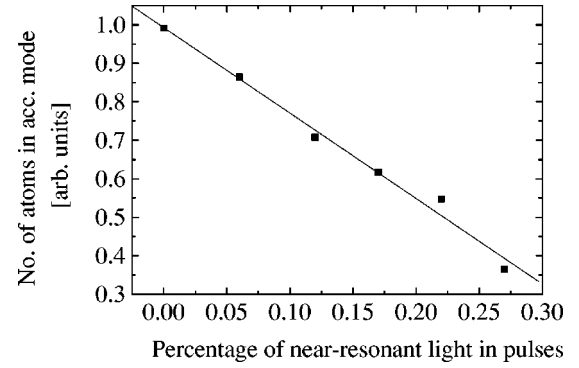


FIG. 14. The number of atoms remaining in the accelerator mode after 30 pulses is plotted for different fractions of near-resonant trapping light in the pulses applied to the atoms. The pulses were separated by 60 μs . The intensity in the standing wave of light was 28 W/cm^2 and its detuning was 6 GHz.

VI. MAXIMUM MOMENTUM GAIN

From the above discussion, it would appear that the accelerator mode could keep increasing its momentum indefinitely once the initial conditions had been satisfied. This in fact is not the case. As stated at the beginning of the theoretical discussion, it was assumed that the atoms do not move significantly during the time of each pulse. As the atomic momentum increases, it reaches a velocity where this assumption is no longer valid and the atoms leave the Raman-Nath regime. When this happens, the movement of the atoms through the standing light wave averages the periodic potential so that the atoms effectively experience a spatially independent potential. Thus the accelerator mode will reach a saturation momentum which becomes smaller as the pulse length increases. Figure 13 shows the accelerator modes with increasing pulse number for three different pulse lengths: 0.5, 0.6, and 0.7 μs . It is clear that the mode saturates after fewer kicks for the longer pulse lengths, as expected. This limit will always be present, even if the atoms are accelerated more quickly by changing the pulse separation or the effective gravity. It is easy to calculate that the atoms will move through half a period on the standing wave in the time of an individual pulse when they reach a speed of ρ_{max} photon recoil velocities given by

$$\rho_{\text{max}} v_r = \frac{\lambda_G}{2\Delta t}. \quad (17)$$

For our experiment, $\lambda_G = 447 \text{ nm}$ is the spatial period of the standing wave, $\Delta t = 0.5 \mu\text{s}$ is the pulse duration, and $v_r = 3 \text{ mm/s}$ is the recoil velocity of the atoms. These lead to $\rho_{\text{max}} \sim 150$. Since all the experiments described in this paper were performed with our minimum pulse switching time of 0.5 μs , the accelerator modes reach the same maximum momentum of about $150\hbar k$. This can be verified by examining the experimental plots.

VII. INDIRECT DEMONSTRATION OF COHERENCE

Before the accelerator mode can be used confidently as a tool in atom-optical experiments, its coherence must be dem-

onstrated. Although we have not yet shown this directly, indirect evidence of its coherence exists through its response to spontaneous emission. In the following experiment, a small amount of the near-resonant $D2F=4 \rightarrow F''=5$ trapping light was pulsed on simultaneously with the kicking pulses from the Ti:sapphire laser. This had the effect of increasing the probability of an atom undergoing excitation and spontaneous emission while in an accelerator mode and thus destroying its phase information. The results are shown in Fig. 14. With such small intensities of on-resonant light, the atoms' excitation probability increases approximately linearly with intensity. Since the excited atoms will decay predominantly to the ground $F=4$ level, where they started, there will not be a drop in the total population detected. The reduction in the number of accelerated atoms must therefore be due to the loss of phase information.

The fact that the accelerator mode is most efficient when decohering factors are kept to a minimum suggests that it is created through a coherent process. Since diffraction itself is coherent, it is not surprising that a process relying on diffraction should also be coherent.

VIII. CONCLUSION

We have demonstrated a technique for imparting large amounts of momentum to cold atoms: the quantum accelera-

tor mode. The mode was realized with cesium atoms in a pulsed standing wave of off-resonant light, which acted on the atomic de Broglie waves as a thin phase diffraction grating. It was found that the pulse interval played a critical role in determining the amount of momentum transferred with each pulse. This was accounted for with a theoretical model in which the evolution of three diffraction orders in the presence of an external gravitational field was considered. The model produced a closed formula which gave excellent agreement with the observed behavior. We also investigated the dependence of the efficiency and momentum transfer of the accelerator mode on the intensity, detuning, polarization, and phase of the light field.

Understanding the role of gravity has enabled the accelerator mode to be controlled by altering the position of the periodic potential with a phase shifter. This control, together with the fact that the process is efficient and appears to be coherent, indicates that the accelerator mode has potential as a versatile tool in atom optics.

ACKNOWLEDGMENTS

This work was supported by the U.K. EPSRC, the Paul Instrument Fund of The Royal Society, and the EU as part of the TMR "Coherent Matter Wave Interactions" network, Contract No. EBRFMRXCT960002.

-
- [1] C.S. Adams, M. Sigel, and J. Mlynek, *Phys. Rep.* **240**, 143 (1994).
 - [2] W. Ertmer and K. Sengstock, *Appl. Phys. B: Lasers Opt.* **69**, 255 (1999).
 - [3] G. Timp, R.E. Behringer, D.M. Tennant, J.E. Cunningham, M. Prentiss, and K.K. Berggren, *Phys. Rev. Lett.* **69**, 1636 (1992).
 - [4] P. Berman, *Atom Interferometry* (Academic Press, San Diego, 1997).
 - [5] M.-O. Mewes, M.R. Andrews, D.M. Kurn, D.S. Durfee, C.G. Townsend, and W. Ketterle, *Phys. Rev. Lett.* **78**, 582 (1997).
 - [6] D.W. Keith, C.R. Ekstrom, Q.A. Turchette, and D.E. Pritchard, *Phys. Rev. Lett.* **66**, 2693 (1991).
 - [7] T.M. Roach, H. Abele, M.G. Boshier, H.L. Grossman, K.P. Zetie, and E.A. Hinds, *Phys. Rev. Lett.* **75**, 629 (1995).
 - [8] M. Kasevich and S. Chu, *Phys. Rev. Lett.* **67**, 181 (1991).
 - [9] J. Lawall and M. Prentiss, *Phys. Rev. Lett.* **72**, 993 (1994).
 - [10] L.S. Goldner, C. Gerz, R.J.C. Spreeuw, S.L. Rolston, C.I. Westbrook, W.D. Phillips, P. Marte, and P. Zoller, *Phys. Rev. Lett.* **72**, 997 (1994).
 - [11] C. Henkel, C.I. Westbrook, and A. Aspect, *J. Opt. Soc. Am. B* **13**, 233 (1996).
 - [12] E.M. Rasel, M.K. Oberthaler, H. Batelaan, J. Schmiedmayer, and A. Zeilinger, *Phys. Rev. Lett.* **75**, 2633 (1995).
 - [13] M. Weitz, B.C. Young, and S. Chu, *Phys. Rev. Lett.* **73**, 2563 (1994).
 - [14] M.K. Oberthaler, R.M. Godun, M.B. d'Arcy, G.S. Summy, and K. Burnett, *Phys. Rev. Lett.* **83**, 4447 (1999).